Effects of strong driving fields in resonant four-wave mixing schemes with down-conversion

S. A. Babin, E. V. Podivilov, and D. A. Shapiro
Institute of Automation and Electrometry, Siberian Branch, Russian Academy of Science, 630090 Novosibirsk, Russia

U. Hinze, E. Tiemann, and B. Wellegehausen
Institut für Quantenoptik, Universität Hannover, Welfengarten 1, 30167 Hannover, Germany

(Received 26 February 1998; revised manuscript received 15 September 1998)

An explicit solution is obtained for the four-wave frequency mixing $\omega_d=\omega_a-\omega_b+\omega_c$ of two strong fields a and c and two weak fields b and d in a four-level system with large Doppler broadening in collinear geometry, where the frequencies of weak fields are nearly equal, $\omega_b\simeq\omega_d$, and the medium is optically thin. Without weak fields there are two independent two-level systems. A pair of weak fields probes two other allowed transitions. A peak of the mixing coefficient as a function of intensity is found around an equal Rabi splitting of both two-level systems. The effect is based on a resonance between two closed cycles of four-wave mixing via different dressed states. Three, four, or six peaks are predicted in the dependence of the mixing coefficient on the frequency of the weak field; two of them are a consequence of averaging over velocities. The model allows an interpretation of the dependence of the output wave power on the intensity and detuning in recent experiments on frequency mixing in sodium vapor. [S1050-2947(99)06401-X]

PACS number(s): 42.50.Hz, 42.62.Fi, 42.65.Ky

I. INTRODUCTION

High-efficiency conversion of radiation by four-wave mixing usually requires pumping of quantum states by megawatt laser pulses. For continuous frequency conversion at essentially lower pumping intensities a higher nonlinear susceptibility is necessary, which is achieved by tuning to resonances. A few experiments on continuous sum frequency mixing have been performed so far, and output signals of about 1 μW in atomic Ne [1] and 10 μW in atomic Na [2] have been obtained at near-resonant conditions.

The use of the resonance is partly hindered by the effect of Doppler broadening, depending on the leading nonlinear process. Within the framework of perturbation theory, it was shown [3] that in Raman-type schemes with difference frequencies, according to $\omega_d=\omega_a-\omega_b+\omega_c$ (see Fig. 1), the role of Doppler broadening decreases. Recently it was proved in atomic neon [4,5] and diatomic molecular sodium, with up-conversion [6] ($\omega_d>\omega_a,\omega_b,\omega_c$) and down-conversion [7] ($\omega_c<\omega_b,\omega_d<\omega_a$), that the difference scheme is more efficient compared with sum frequency mixing. An output power near 0.1–0.2 mW has been reached at exact resonances for all the waves. Moreover, in these resonant four-wave schemes interesting and unexpected power and detuning dependences of the generated field d on the input fields a, b, and c were observed, that could not be related directly to existing analytical calculations of strong-field effects [8,9], because the calculations were restricted to motionless atoms. The experiment displayed, in particular, the saturation of output as a function of the first strong field a and a linear growth with the third strong field c.

The Raman-type scheme, also called the double-Λ scheme, has gained attention concerning lasing without inversion [10] and related topics. Experimentally, such a scheme has been utilized for efficient optical phase conjugation in atomic Na with low-intensity lasers (1 W/cm^2) using coherent population trapping [11]. An efficient frequency conversion of laser pulses in optically thick media (atomic Pb) has been realized by using atomic coherence on a Raman transition accomplished by electromagnetically induced transparency [12]. The effect of Doppler broadening was not so important in both experiments, since nearly degenerate mixing schemes or Rabi frequencies exceeding the inhomogeneous width were used, correspondingly. Also, the Doppler broadening was insignificant for nearly degenerate four-wave mixing in Rb levels [13].

On the other hand, the Doppler broadening is of vital importance for continuous-wave mixing experiments [4–7], and for laser action in the double-Λ scheme [14]. Stimulated by various experiments with gases, different computations

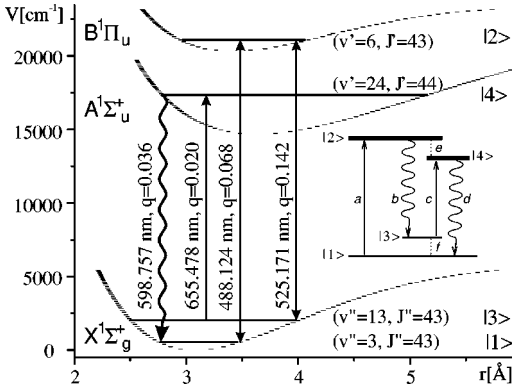

FIG. 1. Considered experimental four-level scheme in Na_2. Four rotational-vibrational levels (v,J) of the states $X\,^1\Sigma_g^+$, $A\,^1\Sigma_u^+$, and $B\,^1\Pi_u$ are coupled by four corresponding fields $\mathbf{E}_\nu$. Wavelengths and Franck-Condon factors q of the involved transitions are given. Inset: the level diagram of a four-level system with four fields. The process of resonant Raman mixing of two strong fields $\mathbf{E}_a$ and $\mathbf{E}_c$ and a weak field $\mathbf{E}_b$ into an output wave $\mathbf{E}_d$. Solid lines show the strong fields a and c; wavy arrows denote the weak fields b and d. Dotted lines display the forbidden transitions e and f. Short-lived upper levels are denoted by wider boxes.

relevant for the experimental situation have been published for Kr [15] and Ne [16], including numerical integration for Maxwellian distribution. The general case of three strong input fields under Doppler broadening can only be handled numerically, while for specific situations, such as for example two strong fields (ω_a, ω_c) and two weak fields with nearly equal frequencies $\omega_b \simeq \omega_d$, compact analytical formulas can also be derived, as recently demonstrated [17]. Such formulas or simplified expressions for limiting cases are helpful for understanding and guiding experiments and will be used in this paper for the interpretation of results obtained in recent four-wave down-conversion experiments [7].

This paper is organized as follows: In Sec. II, the experimental situation is briefly described, and measured parameters of the light and medium are listed. Possible simplification in a theoretical description is noted. Section III introduces the model. Section IV presents the explicit formulas in more general form than in Ref. [17], including arbitrary populations of all the levels. Section V discusses the conversion coefficient as a function of the detuning of the weak field. This dependence has not yet been measured, but seems interesting because it is sensitive to thermal motion. In Sec. VI we compare the intensity dependence given by the formulas with the experiment. In Sec. VII we compare the dependence on strong-field detuning with analytical estimations and the numerical integration over velocity. In Sec. VIII we finally summarize essential aspects of the theoretical consideration and discuss requirements and further directions of experiments.

II. EXPERIMENTAL SCHEME

The four-wave down-conversion mixing under examination is schematically shown by diagram in the inset of Fig. 1. The transitions are denoted by Latin letters, while levels are numbered. The radiation fields are resonant with dipole-allowed transitions between the levels 1, 2, 3, and 4. Experimentally, this scheme has been realized in Na_2 molecular vapor between rotational-vibrational levels of the $X\,^1\Sigma_g^+$, $A\,^1\Sigma_u^+$, and $B\,^1\Pi_u$ electronic states considered as a down-conversion scheme, as indicated in Fig. 1. A similar scheme has also been operated in a He-Ne laser discharge [4,5].

For the operation of a four-wave mixing scheme, three pump fields ($\omega_a, \omega_b, \omega_c$) are needed. Here ω_a is obtained from a single-frequency Ar^+ laser ($\lambda_a = 488$ nm) and ω_c ($\lambda_c = 655$ nm) from a single-frequency ring dye laser. The laser with frequency ω_b is generated by operation of a Na_2 Raman laser between the levels 1-2-3 of Fig. 1 using the Ar^+ laser as a pump. In this way, only two independent pump lasers are needed, and by the operation of the Na_2 Raman laser the frequency ω_b is automatically adjusted to the resonance 2-3. On the operation of continuous Raman lasers in diatomic molecular vapor, see, for example, Ref. [18]. The experimental data used here are obtained in resonant four-wave mixing (RFWM) experiments in an external vapor cell (Na heatpipe) [7], as indicated in Fig. 2. This scheme provides an independent variation of pump intensities.

For optimum frequency mixing, in addition to the frequency condition, a phase-matching condition also has to be fulfilled

$$\omega_d = \omega_a - \omega_b + \omega_c, \quad \mathbf{k}_d = \mathbf{k}_a - \mathbf{k}_b + \mathbf{k}_c, \tag{1}$$

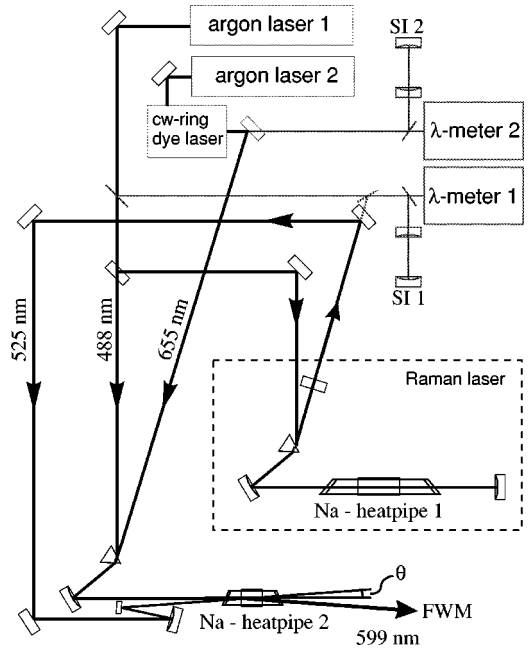

FIG. 2. Experimental setup for resonant four-wave mixing. A part of the field $\mathbf{E}_a$ of single frequency Ar^+-laser 1 is used to pump a Na_2-Raman laser $\mathbf{E}_b$ in heatpipe 1 (dotted box). These fields $\mathbf{E}_a$ and $\mathbf{E}_b$ are mixed with the field $\mathbf{E}_c$ of a cw ring dye laser in heatpipe 2. The generated FWM field $\mathbf{E}_d$ is detected behind heatpipe 2 (noncollinear mixing geometry; see text). Laser frequencies are controlled by λ meters 1 and 2 and scanning interferometers SI 1 and 2.

where $\mathbf{k}_\nu$, $\nu = a, b, c$, and d, is the νth-field wave vector. This is accomplished here in a slight noncollinear mixing geometry induced by atomic D lines, with an angle θ of about 10 mrad between the laser beams ($\mathbf{k}_{a,c}$ and $\mathbf{k}_b$). The angle results in a mixing zone length $L \lesssim 1$ cm, whereas the length of the vapor cloud of the Na heatpipe was about $l \simeq 6$ cm. Therefore, the resonant fourth field d, after being generated in the front part of the pipe, is reabsorbed before reaching the detector. At an operating temperature of the heatpipe of about $T = 740$ K, the characteristic absorption length of the unpumped vapor for the generated radiation is $\alpha_0^{-1} \simeq 2.5$ cm. In the experiment, at pump powers of typically $P_a = 200$ mW, $P_b = 25$ mW, and $P_c = 400$ mW output powers of $P_d = 0.2$ mW are measured. Taking into account the reabsorption in specific geometry, this corresponds to an internally generated power of at least 6 mW and a conversion efficiency $C = P_d / P_a P_b P_c$ as high as 3 W/W^3. For further experimental details, see Ref. [7]. Let us list the experimental parameters significant for the development of adequate theoretical model.

The relaxation constants of levels are $\gamma_2 \simeq \gamma_4 \sim 3 \times 10^8$ s^{-1} and $\gamma_1 \simeq \gamma_3 \sim 3 \times 10^7$ s^{-1}. The lower levels have a purely collisional relaxation, while for the upper ones both radiative and collisional decay are important. The homogeneous width is the convolution of off-diagonal relaxation constants and apparatus broadening, namely, the jitter of laser frequencies and the influence of a small angle between the wave vectors. The estimated value is $\gamma = (3-6) \times 10^8$ s^{-1} for all transitions. The thermal velocity $v_T = \sqrt{2 k_B T / M}$, where k_B is the Boltzmann constant, T is the temperature, and M is the molecular mass, gives the Doppler

widths $k_a v_T = 7.0\times10^9\ \mathrm{s}^{-1}$, $k_b v_T = 6.5\times10^9\ \mathrm{s}^{-1}$, $k_c v_T = 5.2\times10^9\ \mathrm{s}^{-1}$, and $k_d v_T = 5.7\times10^9\ \mathrm{s}^{-1}$. Thus, it is possible to make two simplifications in theory. The difference between k_b and k_d is small (about 12%), and may be ignored as a first approximation. The effective homogeneous width is much less than the Doppler broadening; then the theory can be built up in the Doppler limit $kv_T \gg \gamma$.

Maximum Rabi frequencies Ω_ν can be estimated for experimental focusing scheme $\Omega_a = (1-2)\times10^9\ \mathrm{s}^{-1}$, $\Omega_b = (1-2)\times10^8\ \mathrm{s}^{-1}$, $\Omega_c = (3-6)\times10^8\ \mathrm{s}^{-1}$, and $\Omega_d = (2-4)\times10^7\ \mathrm{s}^{-1}$. Therefore, $\Omega_{b,d} < \gamma < \Omega_{a,c}$; then the approximation of weak fields *b* and *d* and strong fields *a* and *c* looks reasonable.

The estimated level populations are $N_1 \sim 10^{12}\ \mathrm{cm}^{-3}$ and $N_3 \sim 10^{11}\mathrm{cm}^{-3}$, where $N_1 \gg N_3 \gg N_2, N_4$ show that a good approximation is the model of the only lowest level $|1\rangle$ being populated. The absorption of fields *a* and *d* interacting with this level is considerable along the whole heatpipe. However, as mentioned above, the mixing zone length is small, $L < \alpha_0^{-1} < l$. We can consider the mixing problem within the thin medium approximation. Linear absorption of the output wave *d* leads only to an attenuation of the intensity by a constant factor $\exp[-2\alpha_0(l-L)]$ without influencing the analyzed intensity and frequency dependences. That means the spectroscopic problem to compute the nonlinear susceptibility in this case is more important than the optical effects of propagation. Meanwhile, the noncollinearity $\theta \sim 10^{-3}$ is inessential for a spectroscopic treatment.

III. BASIC EQUATIONS

Let us consider the conversion of two strong incident waves $\mathbf{E}_{a,c}$ resonantly interacting with transitions 2-1 and 4-3 and the weak field $\mathbf{E}_b$ near the resonance with transition 2-3 into the output wave $\mathbf{E}_d$ with transition 4-1, according to the inset of Fig. 1. The electric field in the medium is the sum of traveling waves,

$$\mathbf{E}(\mathbf{r},t) = \sum_\nu \mathbf{E}_\nu \exp(-i\omega_\nu t + i\mathbf{k}_\nu \cdot \mathbf{r}), \tag{2}$$

where $\mathbf{E}_\nu$ is the amplitude of the νth field, and $\nu = a,\ b,\ c$, and *d*. The frequency and wave vector of wave *d* satisfy the phase-matching condition (1). Since the cycle 1-2-3-4-1 is closed, the frequency detunings Δ_ν satisfy the condition

$$\Delta_d = \Delta_a - \Delta_b + \Delta_c, \tag{3}$$

where $\Delta_a = \omega_a - \omega_{21}$, $\Delta_b = \omega_b - \omega_{23}$, $\Delta_c = \omega_c - \omega_{43}$, $\Delta_d = \omega_d - \omega_{41}$, and $\omega_{ij} = (E_i - E_j)/\hbar$ are the Bohr transition frequencies.

We can neglect both weak fields to a zeroth-order approximation, i.e., set $\mathbf{E}_{b,d} \to \mathbf{0}$. The complete set of 16 equations for the density matrix of the four-level system reduces, and now allows us to find steady-state populations per unit volume and velocity $\rho_j \equiv \rho_{jj}$ (j:1,2,3,4) and coherences $\rho_{21} \equiv \rho_a \exp(-i\Delta_a t + i\mathbf{k}_a \cdot \mathbf{r})$ and $\rho_{43} \equiv \rho_c \exp(-i\Delta_c t + i\mathbf{k}_c \cdot \mathbf{r})$ of a pair of separated two-level systems:

$$\gamma_1\rho_1 = 2\,\mathrm{Re}(i\Omega_a^*\rho_a) + \gamma_1 N_1(\mathbf{v}),$$

$$\gamma_2\rho_2 = -2\,\mathrm{Re}(i\Omega_a^*\rho_a) + \gamma_2 N_2(\mathbf{v}), \tag{4}$$

$$\Gamma_a\rho_a = i\Omega_a(\rho_1 - \rho_2);$$

$$\gamma_3\rho_3 = 2\,\mathrm{Re}(i\Omega_c^*\rho_c) + \gamma_3 N_3(\mathbf{v}),$$

$$\gamma_4\rho_4 = -2\,\mathrm{Re}(i\Omega_c^*\rho_c) + \gamma_4 N_4(\mathbf{v}), \tag{5}$$

$$\Gamma_c\rho_c = i\Omega_c(\rho_3 - \rho_4).$$

Here $N_j(\mathbf{v})$ and γ_j are the unperturbed population densities per unit velocity interval and relaxation constants of levels $j = 1,\ 2,\ 3$, and 4. For convenience we define the coherences ρ_a and ρ_c so that Ω_a and Ω_c to be real and positive, where $\Omega_\nu = \mathbf{E}_\nu \cdot \boldsymbol{\mu}_\nu / 2\hbar$ is the Rabi frequency of νth transition with the dipole moment $\boldsymbol{\mu}_\nu$. We denote

$$\Gamma_\nu \equiv \gamma_\nu - i\Delta_\nu,$$

where $\gamma_a \equiv \gamma_{12}$ and $\gamma_c = \gamma_{34}$ are the relaxation constants of the coherences, which determine the homogeneous widths. For a medium with thermal motion one should replace $\Delta_\nu \to \Delta_\nu - \mathbf{k}_\nu \mathbf{v}$, where $\mathbf{v}$ is the velocity vector. The unperturbed populations $N_j(\mathbf{v})$ are assumed to have Maxwellian distribution over $\mathbf{v}$,

$$N_j(\mathbf{v}) = \frac{N_j}{(\sqrt{\pi}v_T)^3} \exp\left(-\frac{\mathbf{v}^2}{v_T^2}\right). \tag{6}$$

For motionless particles ($\mathbf{v} \equiv 0$), $N_j(\mathbf{v})$ has to be replaced by constants N_j.

The solutions of Eqs. (4) and (5) are written as

$$\rho_1 = N_1(\mathbf{v}) - \frac{2\Omega_a^2\gamma_a N_{12}(\mathbf{v})}{\gamma_1(\Gamma_{sa}^2 + \Delta_a^2)},$$

$$\rho_2 = N_2(\mathbf{v}) + \frac{2\Omega_a^2\gamma_a N_{12}(\mathbf{v})}{\gamma_2(\Gamma_{sa}^2 + \Delta_a^2)}, \tag{7}$$

$$\rho_a = \frac{i\Omega_a N_{12}(\mathbf{v})\Gamma_a^*}{\Gamma_{sa}^2 + \Delta_a^2};$$

$$\rho_3 = N_3(\mathbf{v}) - \frac{2\Omega_c^2\gamma_c N_{34}(\mathbf{v})}{\gamma_3(\Gamma_{sc}^2 + \Delta_c^2)},$$

$$\rho_4 = N_4(\mathbf{v}) + \frac{2\Omega_c^2\gamma_c N_{34}(\mathbf{v})}{\gamma_4(\Gamma_{sc}^2 + \Delta_c^2)}, \tag{8}$$

$$\rho_c = \frac{i\Omega_c N_{34}(\mathbf{v})\Gamma_c^*}{\Gamma_{sc}^2 + \Delta_c^2},$$

where $N_{ij}(\mathbf{v}) \equiv N_i(\mathbf{v}) - N_j(\mathbf{v})$ is the population difference, and

$$\Gamma_{sa}^2=\gamma_a^2+2\Omega_a^2\gamma_a(\gamma_1^{-1}+\gamma_2^{-1}),$$

$$\Gamma_{sc}^2=\gamma_c^2+2\Omega_c^2\gamma_c(\gamma_3^{-1}+\gamma_4^{-1})$$

are the homogeneous widths including the power broadening.

Weak fields, with amplitudes Ω_b and Ω_d in frequency units, lead to the appearance of coherence between levels belonging to the different two-level systems $\rho_{23}\equiv\rho_b\exp(-i\Delta_b t+i\mathbf{k}_b\cdot\mathbf{r})$ and $\rho_{41}\equiv\rho_d\exp(-i\Delta_d t+i\mathbf{k}_d\cdot\mathbf{r})$ for the allowed transitions, as well as to cross coherences for the forbidden transitions e,f: $\rho_{24}\equiv\rho_e\exp(-i\Delta_e t+i\mathbf{k}_e\cdot\mathbf{r})$ and $\rho_{31}\equiv\rho_f\exp(-i\Delta_f t+i\mathbf{k}_f\cdot\mathbf{r})$, where $\mathbf{k}_e=\mathbf{k}_a-\mathbf{k}_d$, $\mathbf{k}_f=\mathbf{k}_a-\mathbf{k}_b$, $\Delta_e=\Delta_a-\Delta_d$, and $\Delta_f=\Delta_a-\Delta_b$. We neglect the influence of these weak fields on the populations of levels ρ_j. The following set of four algebraic equations appears for the nondiagonal matrix elements ρ_b, ρ_d, ρ_e, and ρ_f in the first-order approximations

$$\begin{aligned}
&\Gamma_b\rho_b-i\Omega_a\rho_f^*+i\Omega_c\rho_e=-i\Omega_b(\rho_2-\rho_3),\\
&\Gamma_d^*\rho_d^*+i\Omega_c^*\rho_f^*-i\Omega_a^*\rho_e=i\Omega_d^*(\rho_4-\rho_1),\\
&\Gamma_e\rho_e-i\Omega_a\rho_d^*+i\Omega_c^*\rho_b=i\Omega_b\rho_c^*-i\Omega_d^*\rho_a,\\
&\Gamma_f^*\rho_f^*+i\Omega_c\rho_d^*-i\Omega_a^*\rho_b=-i\Omega_b\rho_a^*+i\Omega_d^*\rho_c.
\end{aligned}\tag{9}$$

Here $\gamma_b\equiv\gamma_{23},\gamma_d\equiv\gamma_{41}$, and $\gamma_e\equiv\gamma_{24},\gamma_f\equiv\gamma_{31}$ are the constants of relaxation of the coherence of the allowed and forbidden transitions, respectively. The right-hand side in set (9) are given by solutions (7) and (8) for independent two-level systems.

In the limiting case $\Omega_c=\Omega_d=0$ the system is the three-level Λ-scheme 1-2-3. The first and last equations from set (9) remain for coherence ρ_b at allowed transition 2-3 and Raman coherence ρ_f at forbidden transition 1-3,

$$\begin{aligned}
&\Gamma_b\rho_b-i\Omega_a\rho_f^*=-i\Omega_b(\rho_2-\rho_3),\\
&-i\Omega_a\rho_b+\Gamma_f^*\rho_f^*=-i\Omega_b\rho_a^*.
\end{aligned}$$

Terms proportional to the weak field Ω_b on the right side correspond to the two main nonlinear effects of probe field spectroscopy [19]. The first is a population effect, proportional to the population difference $\rho_2-\rho_3$. It includes, in particular, the saturation of population ρ_2 by the strong field Ω_a. The second is the nonlinear interference effect depending on off-diagonal element ρ_a. It describes the mixing of states $|1\rangle$ and $|2\rangle$ by the strong field. The Rabi frequency Ω_a in the left side results in the third effect: the splitting of level $|2\rangle$ by the field. Analogously, at $\Omega_a=\Omega_b=0$ the remaining pair of equations (9) for ρ_d,ρ_f describes the three-level Λ configuration 3-4-1. Generally, at nonzero fields three-level *V* schemes 2-1-4 and 2-3-4 also work and create Raman coherence ρ_e at forbidden transition 2-4.

The Maxwell equation for the generated wave envelope can be reduced to

$$\frac{d\mathbf{E}_d}{dx}=2\pi ik_d\boldsymbol{\mu}_d\langle\rho_d\rangle,\tag{10}$$

where all the input waves are supposed collinear, $\mathbf{k}_a\|\mathbf{k}_c\|\mathbf{k}_b$; x is the coordinate along the common direction of wave vectors; and angular brackets denote the integration over the velocity distribution. In collinear geometry only averaging over the longitudinal velocity is necessary in Eq. (10). If a small angle θ exists between the wave vectors, it can be roughly taken into account as an additional broadening $\sim kv_T\theta$ caused by averaging over the transverse velocity. By doing so we neglect the fine effects of angle tuning.

For a linear polarization of the radiation fields, and assuming weak fields E_d and E_b, Eq. (10) may be written as

$$\frac{dE_d^*}{dx}=-2\pi ik_d\mu_d\langle\rho_d^*\rangle=-\beta E_b-\alpha^*E_d^*,\tag{11}$$

where coefficients α and β depend on the strong fields, and describe the absorption of field $\mathbf{E}_d$ and conversion between two weak fields $\mathbf{E}_b\rightarrow\mathbf{E}_d$, respectively. One can put $\Omega_d=0$ $(\mathbf{E}_d=\mathbf{0})$ into Eq. (9) to obtain the mixing coefficient β or $\Omega_b=0$ $(\mathbf{E}_b=\mathbf{0})$ to find the absorption coefficient α. At the line center under strong fields $\Omega_{a,c}\gg\gamma_\nu$, both the coefficients β and α are of the same order of magnitude, as shown in Sec. IV.

Under the thin medium approximation the generated field is small, $\Omega_d\ll\Omega_b$; then one can neglect the absorption term to find intensities of

$$I_d(L)=|\beta L|^2I_b=\left|\frac{16\pi^2}{c}\chi_d^{\mathrm{NL}}k_dL\right|^2I_aI_bI_c,\tag{12}$$

$$\beta^*=2\pi k_d\chi_d^{\mathrm{NL}}E_aE_c,\tag{13}$$

where I_ν is the intensity, L denotes the length of the medium, and β is represented in terms of the macroscopic nonlinear susceptibility χ_d^{NL}, which depends on the intensities I_a and I_c and contains all odd order coefficients. Within the perturbation theory limit, while Ω_a and Ω_c are much less than Δ or γ_ν, the nonlinear susceptibility χ^{NL} tends to cubic susceptibility $\chi^{(3)}$, which is then no longer intensity dependent. We find the full coefficient β by comparing Eq. (9) with the solution of form (11):

$$\begin{aligned}
\beta=\frac{\pi k_d\mu_d\mu_b}{\hbar}\int d\mathbf{v}\frac{\Omega_a\Omega_c}{D}\Bigg[&(\Gamma_e+\Gamma_f^*)(\rho_2-\rho_3)\\
&-\frac{\rho_a^*}{i\Omega_a}(\Omega_a^2-\Omega_c^2-\Gamma_b\Gamma_e)-\frac{\rho_c^*}{i\Omega_c}(\Omega_c^2-\Omega_a^2-\Gamma_b\Gamma_f^*)\Bigg].
\end{aligned}\tag{14}$$

Here the determinant of set (9) is

$$\begin{aligned}
D=&\Gamma_b\Gamma_e\Gamma_d^*\Gamma_f^*+(\Omega_a^2-\Omega_c^2)^2\\
&+\tfrac{1}{2}(\Omega_a^2+\Omega_c^2)(\Gamma_b+\Gamma_d^*)(\Gamma_e+\Gamma_f^*)\\
&-\tfrac{1}{2}(\Omega_a^2-\Omega_c^2)(\Gamma_b-\Gamma_d^*)(\Gamma_e-\Gamma_f^*),
\end{aligned}\tag{15}$$

the polynomial of the fourth degree in velocity. For the case of collinear propagation we denote the projection of the ve-

locity vector onto the direction of propagation as $v \equiv v_x$. Consider poles of the density matrix corresponding to zeros of determinant D as a function of complex velocity v. For down-conversion $\omega_c < \omega_b, \omega_d < \omega_a$, a pair of poles is located in the upper half-plane and another pair is in the lower half-plane. Each pole close to the real axis specifies the *resonance condition* for interaction between the field and a group of particles with given velocity.

Assuming here that the coherences decay as half the sum of populations (neglecting phase-changing collisions), i.e., $\gamma_a = (\gamma_1 + \gamma_2)/2$, $\gamma_b = (\gamma_3 + \gamma_2)/2$, $\gamma_c = (\gamma_3 + \gamma_4)/2$, and $\gamma_d = (\gamma_1 + \gamma_4)/2$ (for the notations of the levels see the inset of Fig. 1), then the resonance condition factorizes, since Eq. (15) can be rewritten as

$$D = [(\Delta_b' - \Delta_d')^2/4 - (\Omega_{Ra} + \Omega_{Rc})^2] \times [(\Delta_b' - \Delta_d')^2/4 - (\Omega_{Ra} - \Omega_{Rc})^2], \tag{16}$$

where

$$\Omega_{Ra} = \sqrt{\frac{\Delta_a'^2}{4} + \Omega_a^2}, \quad \Omega_{Rc} = \sqrt{\frac{\Delta_c'^2}{4} + \Omega_c^2}$$

are the generalized Rabi frequencies, and

$$\Delta_a' = \Delta_a - \mathbf{k}_a \mathbf{v} + i(\gamma_2 - \gamma_1)/2,$$

$$\Delta_c' = \Delta_c - \mathbf{k}_c \mathbf{v} - i(\gamma_4 - \gamma_3)/2,$$

$$\Delta_b' = \Delta_b - \mathbf{k}_b \mathbf{v} + i\gamma_b,$$

$$\Delta_d' = \Delta_d - \mathbf{k}_d \mathbf{v} - i\gamma_d.$$

Taking into consideration that the phase-matching conditions (1) and (3) give $\Delta_b' + \Delta_d' = \Delta_a' + \Delta_c'$, we see that the resonance condition $D = 0$ occurs when the weak fields become resonant to quasienergy levels

$$\Delta_b' = \left(\frac{\Delta_a'}{2} \pm \Omega_{Ra}\right) + \left(\frac{\Delta_c'}{2} \pm \Omega_{Rc}\right),$$
$$\Delta_d' = \left(\frac{\Delta_a'}{2} \mp \Omega_{Ra}\right) + \left(\frac{\Delta_c'}{2} \mp \Omega_{Rc}\right). \tag{17}$$

Equation (17) defines the resonance frequency of a weak field for a given velocity group of atoms as a function of frequencies and intensities of both strong fields. The spectral dependence of a mixing coefficient on Δ_b or Δ_d has four peaks in the case of monokinetic particles. This is a consequence of the field splitting of levels by strong fields in both two-level systems. Because the positions of resonances strongly depend on the velocity, averaging over velocity (14) can change the spectral dependence of β. The interference of the velocity groups may lead to a variation not only of the amplitude of each peak, but even of their number. In general, the integral over velocity can be evaluated only numerically. However, a compact analytical formula for the mixing coefficient can be obtained for a practically interesting symmetrical case of equal wave vectors, $\mathbf{k}_d = \mathbf{k}_b$. The formula is derived and discussed in Sec. IV.

IV. EXPLICIT FORMULA

Integral (14) for the mixing coefficient can be calculated explicitly at equal relaxation constants of coherences ($\gamma_\nu = \gamma$; $\nu = a$, b, c, and d), exact resonance $\Delta_a = \Delta_c = 0$, and equal wave numbers of the two weak fields $k_b = k_d$. If the wave numbers are not equal, but very close, then the result is also applicable. A small difference $|k_b - k_d| \ll |k_b k_d (k_a - k_b)(k_b - k_c)|^{1/4}$ disturbs function $\beta(\Delta_b, \Omega_a, \Omega_c)$ insignificantly. Even for different relaxation constants of levels, the relaxation of coherences may be equal due to dephasing effects. The applicability of these conditions in experiment is discussed in Sec. II.

In view of the phase-matching condition (3), the weak-field detunings depend on a single parameter $\Delta_d = -\Delta_b \equiv \Delta$. In this symmetrical case the determinant $D(v, \Delta)$ turns to be a function of v^2:

$$D(v, \Delta) = \kappa^4 v^4 - 2\kappa^2 v^2 Q'(\Delta) + Q^2(\Delta), \tag{18}$$

$$Q^2(\Delta) = [z^2 - (\Omega_a - \Omega_c)^2][z^2 - (\Omega_a + \Omega_c)^2],$$

$$Q'(\Delta) = \left(\frac{\epsilon_a^2}{2} - 1\right) z^2 - \Omega_a^2 + \Omega_c^2, \tag{19}$$

$$\epsilon_a = \frac{k_a}{\kappa}, \quad \epsilon_c = \frac{k_c}{\kappa}, \quad \kappa = \frac{1}{2}\sqrt{k_a^2 - k_c^2},$$

where $z = \Delta - i\gamma$ is the extended detuning.

The averaging of coefficient β over velocity is possible for an arbitrary thermal velocity, but the resultant formula in terms of the error function of the complex argument is unwieldy. Then we present a simplified explicit formula in the Doppler limit, when the thermal velocity is large, $\kappa v_T \gg \Omega_\nu, \gamma, \Delta_\nu$:

$$\beta = \frac{\Omega_a \mu_b \Omega_c \mu_d}{\hbar} \frac{\pi^{3/2} k_d}{\kappa v_T} \left\{ \frac{-2izN_{32}}{RQ} + \frac{N_{12}\gamma}{\Gamma_{sa}^2 + \Gamma_{sa} R \epsilon_a + Q\epsilon_a^2} \left[\frac{iz\epsilon_a^2/\gamma + 1}{R} + \frac{4iz\Omega_a^2/\gamma_2 - Q' + \epsilon_a^2 z^2/2}{Q} \left(\frac{1}{R} + \frac{\epsilon_a}{\Gamma_{sa}} \right) \right] \right.$$
$$\left. + \frac{N_{34}\gamma}{\Gamma_{sc}^2 + \Gamma_{sc} R \epsilon_c + Q\epsilon_c^2} \left[\frac{iz\epsilon_c^2/\gamma - 1}{R} + \frac{4iz\Omega_c^2/\gamma_3 + Q' - \epsilon_c^2 z^2/2}{Q} \left(\frac{1}{R} + \frac{\epsilon_c}{\Gamma_{sc}} \right) \right] \right\}, \tag{20}$$

where $R=\sqrt{2(Q-Q')}$, $\mathrm{Re}\,R>0$. We have chosen the branch of two-valued function Q according to the rules

$$\mathrm{Re}\,Q<0 \quad \text{at } P_+<|\Delta|, \quad \mathrm{Re}\,Q\geqslant 0 \quad \text{at } |\Delta|\leqslant P_-,$$

$$\mathrm{sgn}(\mathrm{Im}\,Q)=\mathrm{sgn}\,\Delta \quad \text{at } P_-<|\Delta|\leqslant P_+,$$

where $P_\pm=|\Omega_a\pm\Omega_c|$. If we were to choose another branch of Q, then Q should be replaced by $-Q$ in all formulas. When $k_a\to k_c$ the Doppler limit approximation is broken, and Eq. (20) becomes invalid. However if $\kappa v_T\ll\Omega_\nu,\gamma$, then integration over $\mathbf{v}$ is not necessary, and one can apply the theory for motionless atoms under strong field [8,9].

Consider the limiting cases of Eq. (20). They are important either to compare with experiment or for an interpretation of the phenomenon. When only the lower level $|1\rangle$ is populated ($N_i=0, i\neq 1$) expression (20) reduces to a simple formula. Let us write it for the case of uniform relaxation, i.e., equal relaxation constants γ of populations and polarizations

$$\beta=\frac{\pi^{3/2}}{\hbar\kappa v_T}\frac{N_1 k_d\Omega_a\mu_b\Omega_c\mu_d}{\Gamma_{sa}^2+\Gamma_{sa}R\epsilon_a+Q\epsilon_a^2}\times\left[\frac{\gamma+iz\epsilon_a^2}{R}+\frac{4iz\Omega_a^2+\gamma(\epsilon_a^2z^2/2-Q')}{Q}\left(\frac{1}{R}+\frac{\epsilon_a}{\Gamma_{sa}}\right)\right]. \tag{21}$$

For the domain of weak fields $\Omega_a,\Omega_c\ll\gamma$, the expression for the nonlinear susceptibility, following from Eqs. (13) and (20), can be derived also as the first nonlinear correction of the perturbation theory

$$\chi_d^{(3)}=-\frac{\sqrt{\pi}}{k_a v_T}\frac{\mu_a\mu_b^*\mu_c\mu_d^*}{4\hbar^3}\times\left\{\frac{N_{32}}{(\gamma-i\Delta)^2}+\frac{N_{34}(k_a-k_d)}{(\gamma-i\Delta)(k_b\gamma-ik_c\Delta)}\right\}. \tag{22}$$

Here the conversion coefficient is equal to zero when only the lowest level $|1\rangle$ is populated, since the population N_1 does not enter the expression in the Doppler limit, as well as in up-conversion [3]. The susceptibility is nonzero in the next order of expansion in parameter γ/kv_T.

Using Eq. (20), we can now estimate the relative contributions of different terms in Eq. (11) for a generated wave d. In the strong-field limit $\Omega_a=\Omega_c=\Omega\gg\gamma k_a k_c/\kappa^2$ and exact resonance $\Delta=0$, the mixing coefficient can be estimated as

$$\frac{\beta}{\mu_b}=\frac{\pi^{3/2}k_d\mu_d}{2\hbar\kappa v_T}\sqrt{\frac{\Omega}{\gamma}}\left(\frac{N_{12}\gamma_1}{\gamma_1+\gamma_2}+\frac{N_{34}\gamma_4}{\gamma_3+\gamma_4}-N_{32}\right). \tag{23}$$

As distinct from the perturbative result (22), the mixing coefficient does not turn to zero when only the lower level is populated.

Analogously, the formula for the absorption coefficient α can be derived by comparing set (9) with Eq. (11) and integrating over velocity. The absorption coefficient at the same condition as for Eq. (23) is written as

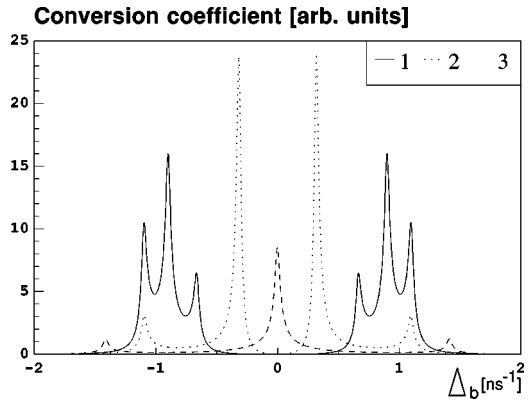

FIG. 3. Conversion coefficient $|\beta|^2\propto I_d/I_aI_bI_c$ in arb. units calculated according to Eq. (21) as a function of detuning Δ_b of the second field at $k_a v_T=7.0$, $k_c v_T=5.2$, and $\gamma=0.02$ for (1) $\Omega_a=1,\Omega_c=0.1$, (2) $\Omega_a=\Omega_c k_a^2/k_c^2=0.5$, and (3) $\Omega_c=\Omega_a=0.5$ (in ns^{-1}).

$$\frac{\alpha}{\mu_d}=\frac{\pi^{3/2}k_d\mu_d}{2\hbar\kappa v_T}\sqrt{\frac{\Omega}{\gamma}}\left(N_{14}-\frac{N_{12}\gamma_2}{\gamma_1+\gamma_2}-\frac{N_{34}\gamma_3}{\gamma_3+\gamma_4}\right), \tag{24}$$

and occurs to be within the same order as β. If only the lower level $|1\rangle$ is populated, then $\alpha/\mu_d=\beta/\mu_b$. Note that the real part of the coefficient α defines the absorption length of field E_d and the applicability of the thin medium approximation. Thus, in the strong-field limit, the approximation is valid, while $\Omega_d\ll\Omega_b$.

V. DEPENDENCE ON THE WEAK-FIELD FREQUENCY

Based on Eq. (21), the dependence of conversion coefficient $|\beta|^2$ vs the detuning Δ_b of the second field is plotted in Fig. 3 at small $\gamma\ll\Omega_a,\Omega_c$ and exact resonance $\Delta_a=\Delta_c=0$. The output intensity is proportional to the conversion coefficient $I_d\sim|\beta|^2$. Hereinafter all the frequencies in figures are given in ns^{-1}. One can see that the number of peaks changes. There are six, four, or three peaks for different relations between the intensities of the strong fields.

Why are there six peaks in conversion coefficient $\eta(\Delta)=I_d/I_aI_bI_c\propto|\beta L|^2$ instead of four, as distinct from the case of motionless atoms? The physical reason for this effect is the interference of light emitted at frequency ω_d by atoms moving with different velocities. If the interference is constructive for some ω_d, then a peak arises in the dependence. By contrast, if it is destructive, then the thermal motion suppresses the mixing. More details will be discussed below.

Expressions (20) and (21) carry information on the results of the interference. We search for maxima of function $\eta(\Delta)$ by looking for minima of Q and R in Eq. (20):

$$\Delta=\pm\Omega_a\pm\Omega_c, \tag{25}$$

where $|Q|$ is minimal, or at

$$\Delta=\pm 2\kappa\sqrt{\frac{\Omega_a^2}{k_a^2}-\frac{\Omega_c^2}{k_c^2}}, \tag{26}$$

provided that

$$\frac{\Omega_a}{k_a^2} \geqslant \frac{\Omega_c}{k_c^2}, \tag{27}$$

where $|R|$ is minimal. As a result, there are six peaks in the dependence, as curve 1 in Fig. 3 shows. At

$$\frac{\Omega_a}{k_a^2} = \frac{\Omega_c}{k_c^2}, \tag{28}$$

minima of both functions $|Q(\Delta)|$ and $|R(\Delta)|$ coincide for detunings $\Delta = \pm 4\Omega_a \kappa^2 / k_a^2$, yielding a four-peak curve. Under this condition the output intensity is highest for the central two peaks, as curve 2 in Fig. 3 displays. Four peaks remain in the dependence, while $\Omega_a k_c^2 / k_a^2 < \Omega_c < \Omega_a$. Finally, at equal Rabi frequencies $\Omega_c = \Omega_a$, the two central peaks of four merge at the center $\Delta = 0$, as curve 3 in Fig. 3 indicates. For $\Omega_c > \Omega_a$ condition (27) is violated; then only four peaks [Eq. (25)] are restored.

The maximal absolute value of the mixing coefficient $|\beta|$ is achieved at detunings given by Eq. (26), when Rabi frequencies of both strong fields obey conditions (28). In the strong-field limit, expression (21) yields

$$|\beta| = \frac{\pi^{3/2} k_d \mu_b \mu_d N_1}{4\hbar \kappa v_T} \frac{(2\kappa)^{1/2}}{(k_a k_c)^{1/4}} \left(\frac{\sqrt{\Omega_a \Omega_c}}{\gamma} \right)^{3/4}, \tag{29}$$

which has the dependence $(\Omega/\gamma)^{3/4}$, in contrast to Eq. (23).

For a qualitative interpretation of the dependence, consider the contribution of particles with given velocity $v_x \equiv v$ into the mixing coefficient β. The resonance condition [the denominator D of the integrand in expression (14) goes to zero] is complied with eigenfrequencies given by Eq. (17). Under the assumption of Sec. IV, the eigenfrequencies take an especially simple form,

$$\Delta(v) = \pm \sqrt{\Omega_a^2 + k_a^2 v^2/4} \pm \sqrt{\Omega_c^2 + k_c^2 v^2/4} - i\gamma. \tag{30}$$

Two upper branches of $\mathrm{Re}\,\Delta(v)$ are shown in Fig. 4(a).

Let us fix a branch $\Delta(v)$ and consider detuning $\Delta = \mathrm{Re}\,\Delta(v_0)$ such that $|d\Delta(v_0)/dv| \geqslant \gamma$, i.e., the derivative with respect to velocity is large enough. Determinant (16) near $v = v_0$ could be written as $D \sim (\mathbf{d}\Delta(v_0)/dv)(v - v_0) - i\gamma$. Integral (14) of $((d\Delta(v_0)/dv)(v - v_0) - i\gamma)^{-1}$ over v around v_0 appears to be small, since contributions of $v < v_0$ and $v > v_0$ cancel each other. Therefore, it is valid to say that radiation emitted by atoms with different velocities experiences the destructive interference; consequently, the mixing and conversion coefficients at this frequency turn to be small.

However, the interference can be constructive, too, if we choose detuning $\Delta = \Delta_R \equiv \mathrm{Re}\,\Delta(v_R)$ such that $d\Delta(v_R)/dv = 0$. In this case the expansion of the determinant starts from a quadratic term $D \sim (d^2\Delta(v_R)/dv^2)(v - v_R)^2/2 - i\gamma$. Integration around $v = v_R$ in Eq. (14) gives the main contribution to β, proportional to $\gamma^{-1/2}$, because the light emitted by atoms with velocity $v > v_R$ and $v < v_R$ add up in phase. All points (v_R, Δ_R) in the (v, Δ) plane, where $d\Delta(v)/dv = 0$, will be called the *return points*. Examples of return points are displayed in Fig. 4(a) as circles. Each results in a narrow peak, shown schematically at the right, near $\Delta = \Delta_R$.

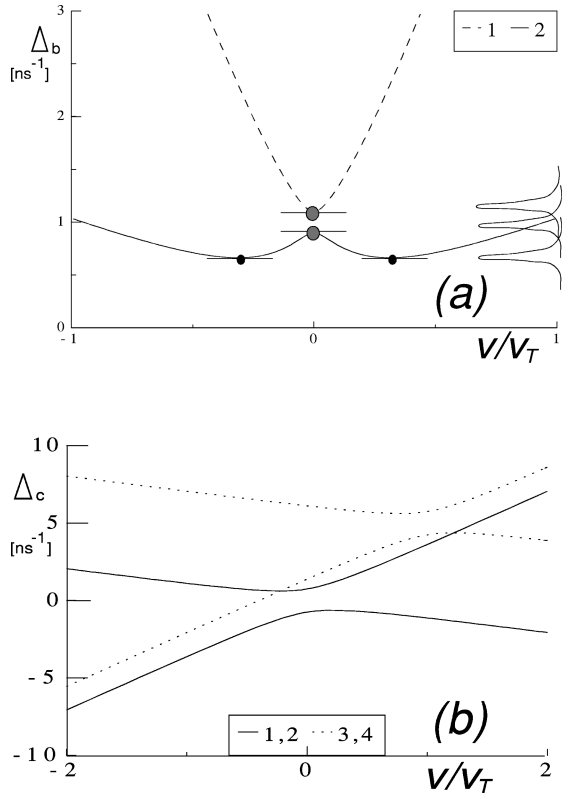

FIG. 4. (a) Resonance condition in the (v, Δ_b) plane at $\Omega_a = 1$, $\Omega_c = 0.1$ (ns^{-1}) for $\Delta_a = \Delta_c = 0$. Two positive solutions $\Delta(v)$ of equation $D(v, \Delta) = 0$ as a function of v/v_T at $\gamma = 0$ calculated by Eq. (30). Curves 1 and 2 correspond to the upper and lower middle signs in the formula. Two other zeros are symmetrical $\Delta \to -\Delta$ with respect to the v axis. Four return points where $d\Delta/dv = 0$ are placed at zero velocities $v = 0$, and four at finite velocity $\kappa v = \pm\sqrt{Q'}$. They are responsible for peaks in the spectrum (shown schematically at the right), because the neighborhood of a return point only gives a constructive contribution to the integral over velocity. (b) Resonance condition in the (v, Δ_c) plane at small Ω_c. Return points corresponding to $\Delta_a = \Delta_b = 0$ (curves 1 and 2) and $\Delta_a = \Delta_b = 6.5$ ns^{-1} (curves 3 and 4).

Equation (30) allows one to find coordinates of the return point. There are four solutions $\Delta_R = \pm\Omega_a \pm \Omega_c$ at $v_R = 0$. The upper pair of these points is shown as big gray circles; the other pair is symmetric about the velocity axis and is not shown in the plot of Fig. 4(a). Additional four return points are placed at

$$\kappa v_R = \pm \sqrt{\left(\frac{\Omega_a k_c}{k_a} \right)^2 - \left(\frac{\Omega_c k_a}{k_c} \right)^2}, \tag{31}$$

whereas the detuning is given by Eq. (26). The velocity has to be real; then condition (27) is necessary. Two of those points are shown by tight black circles in Fig. 4(a). Both have equal detuning in the velocity-frequency plane, and contribute to the same peak shown at the right. Another pair of return points at nonzero velocity is also symmetric about the axis v.

The most interesting phenomenon is the fusion of three return points (one ''gray'' at $v_R = 0$ and two ''black'' at nonzero v_R), when the Rabi frequencies satisfy condition (28). In this special case not only does the first derivative

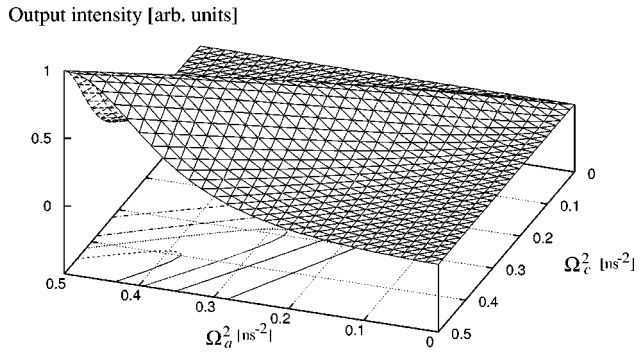

FIG. 5. The intensity of output wave $|\Omega_d|^2 \propto I_d$ as a function of two intensities $I_a \propto \Omega_a^2$, $I_c \propto \Omega_c^2$ of strong fields (in ns^{-2}) at $\gamma = 0.1$. $\Delta = 0$, $k_a v_T = 7.0$, $k_b v_T = 6.5$ (all in ns^{-1}), and $N_2 = N_3 = N_4 = 0$.

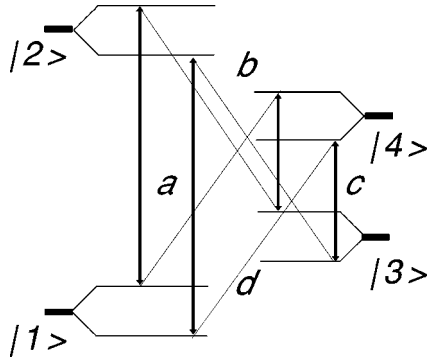

FIG. 6. Scheme of the Rabi splitting of dressed states of motionless atoms. When $\Omega_a = \Omega_c$, the splittings of both two-level systems are equal. Four fields $abcd$ form two closed cycles starting and ending at state $|1\rangle$.

$d\Delta(v_R)/dv$ equal zero, but $d^2\Delta/dv^2$ and $d^3\Delta/dv^3$ also do. The expansion of determinant starts with the fourth power $D \sim (d^4\Delta(v_R)/dv^4)(v - v_R)^4/4! - i\gamma$; then the integration around v_R makes a particularly large contribution proportional to $\gamma^{-3/4}$. The dependence corresponds to Eq. (29) obtained by the explicit formula.

At equal Rabi frequencies $\Omega_a = \Omega_c$ we observe how two return points belonging to the symmetric branches of function $\Delta(v)$ merge at $\Delta = 0$ [in Fig. 4(a) the lower gray circle merges with its mirror image]. This ''fusion'' also increases the height of peak. Unfortunately, this growth is counterbalanced in part by the small numerator in integrand (14) at $\Delta = 0$. The resultant height remains proportional to $\gamma^{-1/2}$ according to formula (23).

Return points (or ''return frequencies'') were introduced in the theory of a probe-field spectrum of a three-level system with large Doppler broadening [20]. The strong field in that theory interacts with a two-level system; then the corresponding determinant is a second-degree polynomial in velocity and detuning. The resonance condition is displayed by two branches of hyperbole in the velocity-detuning plane; then the number of return points is 2 or 0. Consequently, the number of peaks in the probe-field absorption spectrum after averaging over velocity remains equal to 2, as for motionless atoms, or it becomes equal to zero. In the four-level system under consideration the number of peaks in $\beta(\Delta)$ can be more than in motionless case, since the resonance condition $D = 0$ gives four branches of the fourth-order curve in the (v, Δ) plane.

Based on the concept of a return point one can conclude that in the domain of low gas temperature, while $\kappa v_T \ll \sqrt{(\Omega_a k_c/k_a)^2 - (\Omega_c k_a/k_c)^2}$, the additional peaks (26) disappear. The reason is the exponentially small number of particles having as high a velocity as that given by Eq. (31). Thus these additional peaks are sensitive to the velocity distribution in contrast to four main peaks [Eq. (25)].

VI. INTENSITY DEPENDENCE

Reasoning from Eqs. (12) and (21), the output intensity is calculated for complete resonance $\Delta_a = \Delta_b = \Delta_c = \Delta_d = 0$ as a function of both the input intensities of strong fields. The dependence of the normalized output intensity I_d on $I_a = \Omega_a^2 c\hbar^2/2\pi\mu_a^2$ and $I_c = \Omega_c^2 c\hbar^2/2\pi\mu_c^2$ is shown in Fig. 5. The crest near the equal Rabi frequencies is the maximum of output I_d.

To interpret the origin of this maximum qualitatively, let us consider the theory of return points again. We now fix $\Delta = 0$ and find the relation between the Rabi frequency Ω_c and velocity v given by the resonance condition $D = 0$ [Eq. (18)] at $\gamma \to 0$. In the (v, Ω_c^2) plane the resonance condition yields the following parabola:

$$\Omega_c^2 = \Omega_a^2 + \kappa^2 v^2.$$

Analysis analogous to the one presented in Sec. V proves that the peak of $|\beta|$ appears near the return points where $d\Omega_c^2/dv = 0$. The only return point is $v = 0, \Omega_c = \Omega_a$, which leads to a peak in the intensity dependence of output $I_d(I_a, I_c) \propto |\beta(\Omega_a, \Omega_c)|^2$. This peak is formed by particles with nearly zero velocity; then the physical reason for the maximum could be understood within the framework of the picture of dressed states of motionless atoms.

The equal Rabi splitting of levels by strong fields is shown in Fig. 6. Here the frequency ω_b is equal to both the frequencies of the cross-transition from the upper sublevel of level $|4\rangle$ to the upper sublevel of level $|1\rangle$, and of the transition between their lower sublevels, as shown by the thin lines. The equality between frequency ω_d and both transition frequencies between sublevels of 3-2 is concurrently achieved, as also shown by thin lines. Both pathways between all the upper sublevels and all the lower sublevels in Fig. 6 are closed simultaneously, and the fields occur in resonance with the transitions at $\Delta = 0$ only if Rabi frequencies are equal ($\Omega_a = \Omega_c$). Let us call this condition the *Rabi-frequency resonance*.

Such a resonance manifests itself in the RFWM experiment in Na_2 as a saturation of output power. For a discussion of the intensity dependence of $I_d(I_a), I_d(I_c)$, Eqs. (12) and (21) are considered, with the data taken from the experiment, Sec. II.

In Fig. 5 the dependence of the output intensity on the intensities I_a and I_c is given. According to Fig. 5 the Rabi-frequency resonance $\Omega_a = \Omega_c$ results in a peak in the dependence $I_d(I_a)$ at fixed I_c, and in a peak in the dependence $I_d(I_c)$ at fixed I_a. The width of the peak is defined by the effective γ. Since in the experiment γ was very large, the peak was wide. For a high relaxation constant, Eq. (21) gives

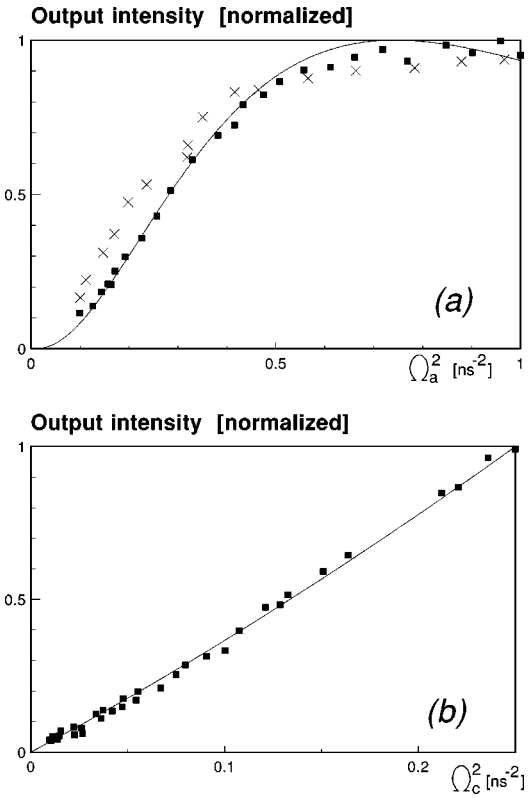

FIG. 7. (a) Output intensity $I_d \propto |\beta|^2$ (arb. units) as a function of the intensity $I_a \propto \Omega_a^2$ at $\Omega_c^2 = 0.25$ ns^{-2}, $\Delta = 0$, and $\gamma = 0.6$ ns^{-1}. Experimental data [7] are taken at two different values of I_b: 25 mW (boxes) and 3 mW (crosses), normalized to equal values at $\Omega_a^2 = 0.5$ ns^{-2}. (b) Output wave intensity as a function of $I_c \propto \Omega_c^2$ at $\Omega_a^2 = 1$ ns^{-2}. Boxes correspond to experiment.

a smooth curve $I_d(I_a)$, shown in Fig. 7(a), that looks like a ''saturation.'' The maximum in this dependence $I_d(I_a) \propto |\beta|^2$ is shifted to higher intensities with respect to the Rabi-frequency resonance, because the output intensity at small I_a increases as I_a^3 [Eq. (21)] until it falls down. Such a run of the curve was measured for different values I_b varied by one order, as shown by crosses and boxes. At the same parameters there is no peak in the dependence on the other strong-field intensity $I_d(I_c)$ both in theory and experiment [Fig. 7(b)]. The reason for this is that the maximum intensity of field c available in the experiment was less than necessary to detect the peak, i.e., $\Omega_c < \Omega_a$.

Within the domain of small intensity, asymptotic experimental data are absent. This does not allow us to verify the features of perturbation theory. However, experimental points show that the function $I_d(I_a)$ may not be entirely linear near $I_a = 0$. In addition, the asymptotics near $I_c = 0$ is approximately linear in contrast to the previous case. Both asymptotics agree with the explicit formula (21). Thus a good agreement of the model with experiment is demonstrated qualitatively, and even quantitatively within an accuracy of experimental points, as Fig. 7 shows. Simultaneously the experiment differs from the perturbative picture [Eq. (22)].

VII. DEPENDENCE ON THE STRONG-FIELD FREQUENCY

Fortunately, the dependence $I_d(\Delta_c, \Delta_a)$ on the detuning of the strong fields was measured under the condition $\Delta_b \simeq \Delta_a$, without independent variation of Δ_b. This corresponds to the resonant operation of the Raman laser (remember that ω_b is generated as a Stokes-type Raman laser pumped by the laser ω_a). In such experiments it was observed that the maximum point of the detuning curve $I_d(\Delta_c)$ does not depend practically on the detuning of the Raman laser with $\Delta_b \simeq \Delta_a$, and lies around $\Delta_c = 0$. Let us analyze the dependence of the conversion coefficient on the third field detuning Δ_c. Here the determinant (15) is not biquadratic, so the following spectra are obtained by numerical integration.

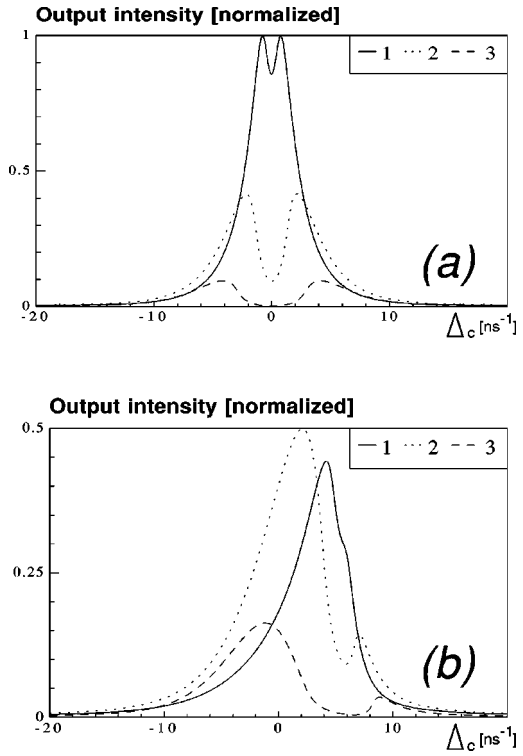

FIG. 8. (a) Output intensity I_d (arb. units) vs detuning Δ_c at several amplitudes of wave a: $\Omega_a = 1$ (curve 1), 2 (curve 2), and 4 (curve 3); $N_3 = 0.1N_1$, $N_2 = N_4 = 0$, $\gamma = 0.6$, $k_a v_T = 7.0$, $k_b v_T = 6.5$, and $k_c v_T = 5.2$; $\Omega_b = 0.1$ and $\Omega_c = 0.5$; and $\Delta_a = \Delta_b = 0$. (b) The same at $\Delta_a = \Delta_b = 6.5$. The maximum point moves toward $\Delta_c = 0$ with growing Ω_a.

Calculations were carried out with the help of a simple program, which integrates the solution of the density matrix equations (9) over velocity by the Simpson method. For exact resonance $\Delta_a = \Delta_c = 0$ and uniform relaxation γ in the Doppler limit, the numerical result coincides with the explicit formula (21). In the general case the input parameters are the following: ten relaxation constants (four for levels and six for coherences), three detunings and wave vectors, three intensities (of two strong fields and one weak field), four unperturbed populations, and four Einstein coefficients. We also set the populations of upper levels $|2\rangle$ and $|4\rangle$ equal to zero, since the temperature in the experiment was much less than the energy interval between electronic states of the molecule.

Figure 8(a) shows the dependence of the output intensity I_d on the detuning Δ_c. The Rabi frequency of the first field is doubled with increasing curve number; that is, $\Omega_a = 1 \times 10^9$ s^{-1} for curve 1, 2×10^9 s^{-1} for curve 2, and 4×10^9 s^{-1} for curve 3 at fixed $\Omega_c = 0.5 \times 10^9$ s^{-1}. We see

the Rabi splitting of the line. The distance between components is nearly proportional to the first wave amplitude if $\Omega_a \gg \Omega_c$. Figure 8(b) displays the same three cases for the detuned first and second waves by the Doppler width $\Delta_a = \Delta_b = k_b v_T$. Now the dip is centered approximately at Δ_a, but the main peak is close to zero detuning. Its position depends on Rabi splitting, and under the stronger driving field $\Omega_a \gg \Omega_c$ the position may become negative. When $\Omega_a \equiv \Omega_c$ the two components merge into one centered approximately at $\Delta_c \simeq \Delta_a$.

To interpret the spectral dependence, let us put the Raman laser condition $\Delta_b = \Delta_a$ into Eq. (16). For a qualitative analysis we set $\Omega_c = \gamma = D = 0$; then, the quadratic equation obtained,

$$\Delta_c^2 - \Delta_c((2k_d - k_a)v + \Delta_a) + \Delta_a k_d v - k_d(k_a - k_d)v^2 - \Omega_a^2 = 0, \qquad (32)$$

describes a hyperbole in (v, Δ_c) plane. Detuning Δ_c satisfying Eq. (32) is shown in Fig. 4(b) as a function of the velocity v/v_T. The solid hyperbole corresponds to the exact resonance $\Delta_a = 0$, whereas the dotted one refers to the detuning $\Delta_a \simeq k_b v_T$. The return points of curves 3 and 4 are shifted to the right. The dependence on Δ_c has two peaks, because there are two return points

$$v = \frac{\Delta_a}{k_a} \mp \frac{\Omega_a(2k_d - k_a)}{k_a\sqrt{k_d(k_a - k_d)}},$$

$$\Delta_c = \frac{k_d}{k_a}\Delta_a \pm \frac{2\sqrt{k_d(k_a - k_d)}}{k_a}\Omega_a \qquad (33)$$

located in the (v, Δ_c) plane, as for a three-level system [20], coupled with strong and probe fields at the adjacent transitions. The positions of return points reflect resonances in the dependence $I_d(\Delta_c)$. The coordinate of the dip in the numerical calculation [Fig. 8(b)] is proportional to Δ_a, whereas the distance between the peaks is proportional to Rabi frequency Ω_a.

Figure 9(a) shows the contour $I_d(\Delta_c)$ at fixed intensities but different detuning values of the Raman laser $\Delta_a = \Delta_b = (1-2)k_b v_T$. The contour for each case consists of a wide main peak and a narrow satellite. The satellite vanishes with an increase in Raman detuning. The width of the main peak is close to the Doppler one, its position being almost independent of the detuning as in the experiment. Figure 9(b) illustrates the comparison of the position in experiment and calculation. The present theory agrees with experimental points qualitatively, since the position of the maximum is near the line center and almost independent of detuning Δ_a, as distinct from the perturbation theory. The perturbation theory gives quite a different dependence, namely, the peak shifts proportionally to Raman detuning, $\Delta_c \simeq k_c \Delta_a / k_b$ for down-conversion as well as for up-conversion [3].

The only principle distinction between theory and experiment is a dip in the center at the exact resonance. Two components appear analogous to the Autler-Townes doublet in a three-level system, as mentioned in Ref. [9]. Such a large splitting should be resolvable under actual experimental accuracy. However, a smooth contour without a dip had been observed. The splitting is first apparent at the exact resonance, while experimental data are available only for $|\Delta_a| \geqslant k v_T/2$. In the experiments the shifted component will be difficult to detect [Fig. 9(a)]. Several reasons for ''washing off'' the dip are also possible. In the experiment the intensity of wave *b* is already powerful enough to give Rabi frequencies comparable to the relaxation rates $\gamma_b \sim \gamma$, which does not fulfill assumptions of the above theory. The differences in Rabi frequencies for transitions between magnetic sublevels can smooth the total contour, too.

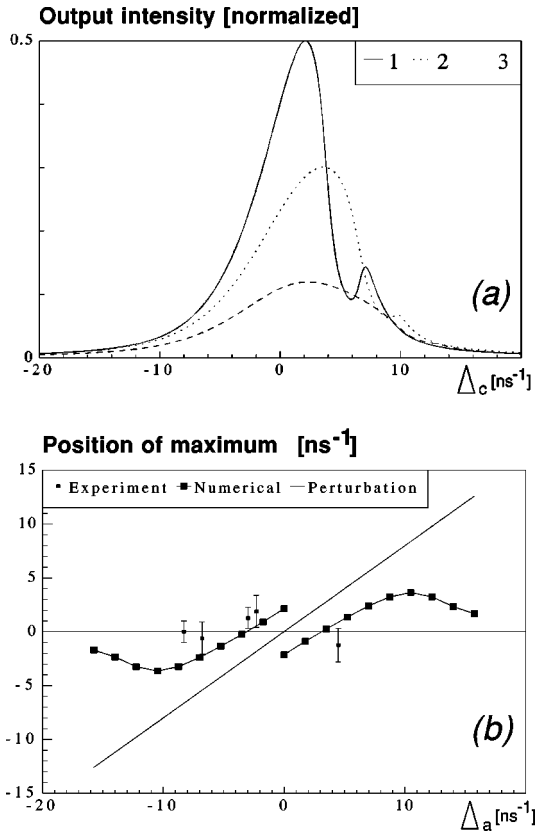

FIG. 9. (a) Output intensity I_d (arb. units) vs the detuning Δ_c at different values of the detuning $\Delta_a = \Delta_b = 6.5$ (curve 1), 10 (curve 2), and 14 (curve 3); $N_1 = 1.0, N_3 = 0.1$, $N_2 = N_4 = 0$, $\gamma = 0.6$, $k_a v_T = 7.0$, $k_b v_T = 6.5$, and $k_c v_T = 5.2$; $\Omega_a = 2$, $\Omega_b = 0.1$, and $\Omega_c = 0.5$. (b) Position Δ_c of maximum of contour $I_d(\Delta_c)$ vs detuning of the Raman laser $\Delta_b = \Delta_a$: perturbation theory, numerical calculations for the above parameters, and experimental points [7].

VIII. CONCLUSIONS

Let us summarize the treatment of strong-field effects for RFWM in Doppler-broadened media. The theory is developed for Raman-type down-conversion (double Λ) schemes with strong-weak-strong-weak field topology, where the output wave is generated by the mixing of three input waves. An explicit solution for the symmetrical case of equal relaxation constants ($\gamma_\nu = \gamma, \nu = a,b,c,d$) and wave numbers of weak fields ($k_b = k_d$) has been obtained. The analysis of the resultant formula gives a clear picture of basic strong-field effects in such a scheme. A multipeak (up to six) structure for the conversion coefficient versus detuning of the weak field Δ_b has been revealed; four of the peaks are a conse-

quence of Rabi splitting of levels by strong fields, and two others appear through constructive interference of light emitted by different velocity groups. At equal Rabi frequencies of the strong fields $\Omega_a=\Omega_c$, two peaks collapse into one resonance maximum at the line center. Such a resonance condition is a result of the interference of RFWM cycles involving different Rabi sublevels at a complete resonance $\Delta_\nu=0$. It determines the maximum conversion coefficient.

This effect can be verified experimentally, since the assumptions of the theory agree with the conditions of Ref. [7]. It is shown that, for $\Omega_a^{\max}>\Omega_c^{\max}$ realized in the experiment, the resonance condition for strong fields leads to a saturation of the output power versus the intensity of the first field $I_d(I_a)$. At the same time there is no saturation of the dependence $I_d(I_c)$ in accordance with the theory. Moreover, the asymptotics for these two curves are quite different: $I_d\propto I_a^3$ at $I_c=\text{const}$ for smaller I_a and $I_d\propto I_c$ at $I_a=\text{const}$, since the two strong fields interact with different lower levels having different populations, $N_1\gg N_3$.

Another significant feature of the experiment is the unexpected dependence of the output power versus the detuning of strong field $I_d(\Delta_c)$: it has a large width (comparable to the Doppler one), and the position of its maximum is not sensitive to the detuning of the Raman laser $\Delta_b\simeq\Delta_a$ used as a source of second (weak) pump field. This is in contradiction with the perturbation theory. To explain such a behavior, numerical calculations involving variations of strong-field detuning have been explored. It is shown that the contour $I_d(\Delta_c)$ is also a subject of Rabi splitting induced by the strongest field Ω_a. In the general case, the contour has two components of different height and width, and the splitting is proportional to the Rabi frequency Ω_a. At $\Omega_a\simeq 2\times 10^9\ \text{s}^{-1}$, which is inside the domain of the estimated experimental parameters, the main peak has a width close to the Doppler width, and its maximum lies near the line center independently of the detuning of $\Delta_b\simeq\Delta_a$, as in the experiment.

The main uncertainty in the experiment is a possible mismatch in the frequencies of the pump and Raman fields ($|\Delta_b|-|\Delta_a|\sim\Omega_a$), which does not allow one to compare in detail the shape of the contour $I_d(\Delta_c)$ with the theory, since it is very sensitive to the above mismatch. One can see that the scale of the detuning axis in Fig. 3 is less than that in Figs. 8(a) and 8(b) by an order of magnitude. That means a much higher sensitivity to the weak-field detuning Δ_b compared to the strong-field detuning Δ_c. Nevertheless, there is strong evidence of agreement between various experimental data with the theory within a domain of self-consistent parameters, which is a good demonstration of the model's validity.

To compare theory and experiment in further detail, as well as to test some predicted dependences, it will be necessary to reduce the jitter of the lasers and to increase the accuracy of the frequency adjustment. If the Raman laser is used to generate the second wave, some tunability inside the Raman gain contour is necessary to test the dependence on the weak-field frequency. When all the frequencies are resonant with the corresponding transition within an accuracy determined by the least relaxation constant $\gamma=\min\gamma_\nu$, the fundamental condition of equal Rabi frequencies of the strong fields $\Omega_a=\Omega_c$ plays the main role for efficient conversion. If $\Omega_a\neq\Omega_c$, one has to adjust the frequency of the weak field to one of the four shifted resonances $\Delta_b=\pm\Omega_a\pm\Omega_c$. Here we expect the maximum conversion coefficient at $\Omega_a=\Omega_c k_a^2/k_c^2$, as curve 2 in Fig. 3 shows.

In principle, the four-wave mixing scheme discussed above may also be considered as a $\chi^{(3)}$ optical parametric generator, analogous to the well-known $\chi^{(2)}$ optical parametric generator, where two pump fields generate a signal field and an idler field. Here the two strong pump fields ω_a and ω_c drive two weaker fields ω_b and ω_d. For both fields ω_b and ω_d, exponential growth should occur, which for the field ω_b is manifested by Raman lasing. In fact, if the field ω_d is generated within the resonator of the Raman laser, the scheme may already be considered as a $\chi^{(3)}$ singly resonant optical parametric oscillator. It should therefore also be of interest to realize feedback and oscillation for the fourth wave, corresponding to the double-resonant optical parametric oscillator. Theoretical and experimental investigations in this direction will be made.

ACKNOWLEDGMENTS

We are grateful to A. K. Popov, M. G. Stepanov, and A. A. Apolonsky for fruitful discussions on theory and experiment, respectively. This work was partially supported by RFBR Grants Nos. 96-02-00069G and 96-15-96642, and by Deutsche Forschungsgemeinschaft Grant No. WE 872/18-1.

[1] V. Klementiev, Y. Matyugin, and V. Chebotaev, Pis'ma Z. Éksp. Teor. Fiz. **24**, 8 (1976) [JETP Lett. **24**, 5 (1976)].

[2] L. Bolotskikh *et al.*, Appl. Phys. B: Photophys. Laser Chem. **35**, 249 (1984).

[3] A. Budnitsky and A. Popov, Opt. Spektrosk. **29**, 1032 (1970) [Opt. Spectrosc. **29**, 550 (1970)].

[4] T. Mueller-Wirts, M. Dernier, A. Popov, and B. Wellegehausen, in *International Quantum Electronics Conference*, Technical Digest Series Vol. 19 (OSA, Washington, DC, 1994), p. 25, paper QMG7.

[5] B. Wellegehausen and T. Mueller-Wirts, in *15th International Conference on Coherent and Nonlinear Optics. Technical Digest* (Vavilov Optical Institute, St. Peterburg, 1995), p. 79.

[6] A. Apolonsky *et al.*, Appl. Phys. B: Photophys. Laser Chem. **64**, 435 (1997).

[7] S. Babin, U. Hinze, E. Tiemann, and B. Wellegehausen, Opt. Lett. **21**, 1186 (1996).

[8] A. Popov, Izv. Ross. Akad. Nauk, Ser. Fiz. **60**, 99 (1996).

[9] D. Coppeta, P. Kelley, P. Harshman, and T. Gustavson, Phys. Rev. A **53**, 925 (1996).

[10] O. Kocharovskaya and P. Mandel, Phys. Rev. A **42**, 523 (1990).

[11] P. Hemmer *et al.*, Opt. Lett. **20**, 982 (1995).

[12] M. Jain *et al.*, Phys. Rev. Lett. **77**, 4326 (1996).

[13] J. Lin, A. Rubiera, and Y. Zhu, Phys. Rev. A **52**, 4882 (1995).
[14] C. Peters and W. Lange, Appl. Phys. B: Photophys. Laser Chem. **62**, 221 (1996).
[15] J. Petch, C. Keitel, P. Knight, and J. Marangos, Phys. Rev. A **53**, 543 (1996).
[16] A. Popov and S. Myslivets, Kvant. Elektron. (Moscow) **24**, 1033 (1997) [Quantum Electron. **27**, 1004 (1997)].
[17] S. Babin, E. Podivilov, and D. Shapiro, Pis'ma Zh. Éksp. Teor. Fiz. **66**, 777 (1997) [JETP Lett. **66**, 816 (1997)].
[18] B. Wellegehausen, IEEE J. Quantum Electron **15**, 1108 (1979).
[19] S. Rautian and A. Shalagin, *Kinetic Problems of Non-Linear Spectroscopy* (Elsevier, Amsterdam, 1991).
[20] O. Bykova, V. Lebedeva, N. Bykova, and A. Petukhov, Opt. Spektrosk. **53**, 171 (1982) [Opt. Spectrosc. **53**, 101 (1982)].